

## Wireless sensor node powered by aircraft specific thermoelectric energy harvesting

D. Samson<sup>a,\*</sup>, M. Kluge<sup>a</sup>, Th. Becker<sup>a</sup>, U. Schmid<sup>b</sup>

<sup>a</sup> EADS Innovation Works, Sensors, Electronics & Systems Integration, Willy-Messerschmidt-Strasse, 81663 Munich, Bavaria, Germany

<sup>b</sup> Department for Microsystems Technology, Institute of Sensor and Actuator Systems, Vienna University of Technology, Floragasse 7, 1040 Vienna, Austria

### ARTICLE INFO

#### Article history:

Available online 25 December 2010

#### Keywords:

Energy harvesting  
Thermoelectric generator  
Phase-change material  
Power management  
Wireless sensor network

### ABSTRACT

An energy autonomous wireless sensor system consisting of an energy harvesting power source, an energy management unit and a low power wireless sensor node is tested for aircraft applications. The autonomous power source combines aircraft specific outside temperature changes with a thermoelectric generator (TEG) and a heat storage unit. The temperature difference generated with the latter component artificially at the TEG is used to power the sensor node by thermoelectricity. Additionally, a high efficient low input voltage power management circuit is necessary to store the generated energy and to convert it to higher voltage levels needed to operate the sensor. The experimental data are compared with results from numerical simulation models to predict the energy conversion in the heat storage – TEG system. A new TEG prototype is tested and the energy output is improved by 14%. The power management storage capacitors are adapted to the available energy, thereby increasing storage voltage and conversion efficiency. Doing so, the efficiency of the complete system can be increased by around 50%.

© 2011 Elsevier B.V. All rights reserved.

## 1. Introduction

The overall operating costs of civil aircraft per flight hour can be subdivided into 4 major areas such as depreciation, flight crew salaries, fuel costs and maintenance, whereas the latter sums up to about 18% [1,2]. Therefore, the introduction of a health monitoring system (HMS) could help to reduce this large part associated with the maintenance costs. For example, with a reliable HMS today's scheduled maintenance could be replaced by maintenance on demand or today's time expensive visual checks in remote areas could be replaced by a remote check from a comfortable position. Autonomous wireless sensor nodes powered by a smart energy harvesting approach are essential for the realization of such a HMS of small wireless sensor nodes due to two main reasons. First, the autonomy reduces the weight as well as the complexity of the whole system as no conventional cabling for data and power transmission is needed. Secondly, this approach makes regular maintenance checks at the sensor nodes to replace local energy sources like batteries obsolete. An energy harvesting powered wireless sensor node consists of three key components: the independent energy source, the power management system and the wireless sensor unit (see also Fig. 1). This article focuses on the

realization of the energy source, but considers in addition main aspects for the design and the realization of the power management.

As the aircraft envelop experiences huge and fast temperature changes during take-off and landing energy harvesting with a thermoelectric generator (TEG) is regarded as a promising approach. First tests of a complete autonomous sensor node were performed in a climate chamber simulating a 60 min short range flight [3]. The energy harvesting power supply worked reliable and the generated energy is sufficient to power a sensor for three additional flights. Energy directly generated by the TEG was approximately 6 mW h with a total conversion efficiency of the power management of about 20%. Based on these results, several improvements are done on component level: the TEG is replaced by a custom-built device from Marlow industries, inc., with a higher figure-of-merit Z in the investigated temperature range and the storage capacity of the power management circuit is reduced to provide a higher storage voltage and hence, an enhanced conversion efficiency.

## 2. Technical details

In this study, thermoelectric conversion is applied for energy harvesting purposes in an aircraft making use of a fuselage temperature varying between +20.4 °C ( $T_h$ ) and –21.8 °C ( $T_c$ ). A typical short-range flight temperature profile of an aircraft hull consists of take-off and climbing with temperature changes from 20.4 °C to –21.8 °C in around 14 min, followed by a 30 min cruise flight

\* Corresponding author. Tel.: +49 89 607 25512; fax: +49 89 607 24001.

E-mail addresses: dominik.samson@eads.net, mail@dominiksamson.de (D. Samson), martin.kluge@eads.net (M. Kluge), thomas.becker@eads.net (Th. Becker), ulrich.schmid+e366@tuwien.ac.at (U. Schmid).

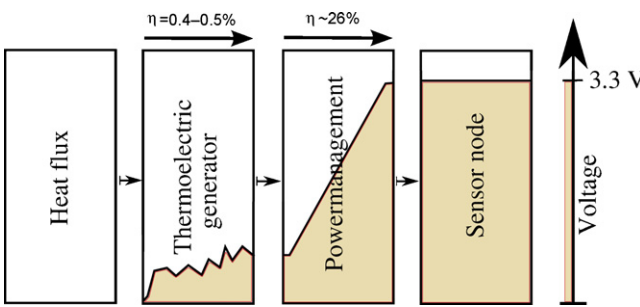


**Fig. 1.** Schematic of the energy harvesting powered sensor system. Energy flux and conversion efficiencies of the different components are indicated. The different voltage levels in the components are also included (TEG: changing low voltage, power management: voltage step-up from low to 3.3 V, sensor node at 3.3 V constant).

at  $-21.8^{\circ}\text{C}$  and finally the descend, landing and taxiing with temperature changes contrary to the take-off phase followed by 30 min ground time at  $20.4^{\circ}\text{C}$  [3]. A TEG connected at one side to the inner fuselage whereas a heat storage unit filled with 10 g water is attached at the other side of the TEG experiences an artificial temperature gradient  $\Delta T$  and thus generates electrical power [4]. Water is an appropriate choice for heat storage purposes, as it offers a phase change between  $T_h$  and  $T_c$  increasing the storable quantity of heat  $Q$  significantly. Additionally, it is expected that simple salt (e.g. sodium chloride) could be added to the water shifting the phase change point between  $0^{\circ}\text{C}$  and  $-21.2^{\circ}\text{C}$  [5], which should allow usage of the latent heat storage ability of the water/salt mixture even at airport ground temperatures below  $0^{\circ}\text{C}$ .

A power management is necessary to convert the variable low voltage input from the TEG ( $<1.5\text{ V}$ ) to a constant voltage level of 3.3 V used by the sensor. Electrical energy harvested above the actual need is stored in capacitors to buffer power peaks and unsupplied parking positions of the aircraft. With the initial power management prototype [6] an overall conversion efficiency of about 19% is reached [3].

The low power wireless sensor unit, consisting mainly of a Texas Instruments MSP430 series microcontroller and a 2.4 GHz IEEE 802.15.4 RF transceiver (Texas Instruments CC2420) [7]) is equipped with a crack wire sensor and consumes  $\sim 189\text{ }\mu\text{W}$  at 3.3 V.

### 3. Simulation model

With a numerical simulation model the impact of different containments for the PCM can be easily evaluated in advance. Furthermore, TEG parameters can be changed to study the influence of generators with different figure-of-merits  $Z$  on the total performance of the system. For the simulation model the software tool COMSOL with its heat transfer module and the heat equation  $\rho \cdot C_p(\partial T/\partial t) + \nabla^2 Q = 0$  is used, whereas the boundary conditions for the simulated hull temperatures during the flight are as described in Section 2.  $\dot{Q}$  is the heat flux,  $C_p$  the specific heat capacity and  $\rho$  the density of phase-change material. The maximum power output generated at the TEG is given by  $P = (\alpha \Delta T)^2/4R_i$ , where  $\alpha$  is the Seebeck-coefficient of the TEG and  $R_i$  is its internal electrical resistance. Yet, the electrical current causes the Peltier-related heat transport  $\dot{Q}_p = \alpha \cdot T_h \cdot I_c$ , where  $I_c$  denotes the electric current through the generator and hence, influences  $\Delta T$ . Therefore, it is necessary to include this correlation between  $\Delta T$  and  $I_c$  in the simulations. This is done by implementing the varying thermal conductivity  $\lambda_{\text{TEG}}$  depending on  $I_c$  as follows:

$$\lambda_{\text{TEG}} = \lambda_{\text{cond.}} + \lambda_{\text{Pelt.}} + \lambda_{\text{Joule}} \quad (1)$$

where  $\lambda_{\text{cond.}}$  is assumed to be constant for small  $\Delta T$  variations,  $\lambda_{\text{Pelt.}} = l \cdot \dot{Q}_{\text{Pelt.}}/(A \cdot \Delta T) = l \cdot \alpha^2 \cdot T_h/A \cdot (R_i + R_{\text{load}})$  and  $\lambda_{\text{Joule}} = -[l \cdot \dot{Q}_{\text{Joule}}/A \cdot 2 \cdot \Delta T] = -(l \cdot 2 \cdot T \cdot R_i)/(A \cdot 2 \cdot (R_i + R_{\text{load}})^2)$  (negative because  $\dot{Q}_{\text{Joule}} \approx -\dot{Q}_{\text{Pelt.}}$ ). In this context,  $R_{\text{load}}$  denotes the electrical resistance of the external load,  $l$  is the thickness of the TEG and  $A$  the area of the TEG. Doing so, the feedback of different electrical loads on the performance of the TEG is simulated. It is also possible to optimize  $\lambda_{\text{TEG}}$  in such a way that in a predefined time (e.g. for a short flight of 88 min) the complete stored heat  $Q$  is consumed by the TEG, defined as  $T_{\text{PCM}} - T_c < 1$ . Typically, the uncertainty associated with the simulated energy output compared to the experimentally determined quantity is  $<7\%$ .

The mismatch between simulation and experiment in Fig. 2 probably arises from the effect of natural convection: When the PCM heats up, the bottom layers of the PCM start to melt and the cold ice swims up. At first this reduces the available temperature gradient at the TEG and explains the reduced power output in comparison with the simulation in Fig. 2 just before  $t = 70\text{ min}$ . After  $t = 70\text{ min}$  the point is reached when it becomes important that cold

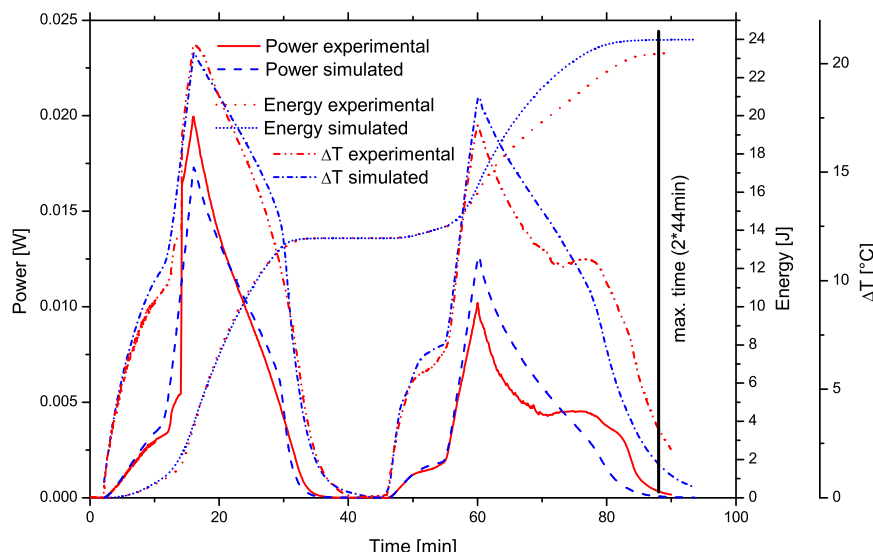


**Fig. 2.** Comparison of simulated and measured output power as well as the extracted energy levels from the thermoelectric harvesting device. The strong discrepancy in the corresponding characteristics above 60 min is attributed to the natural convection in the water-filled containment during the experiment, which is not included in the simulations. The temperature difference  $\Delta T$  between hull temperature and TEG-PCM containment contact point is also included in the figure.

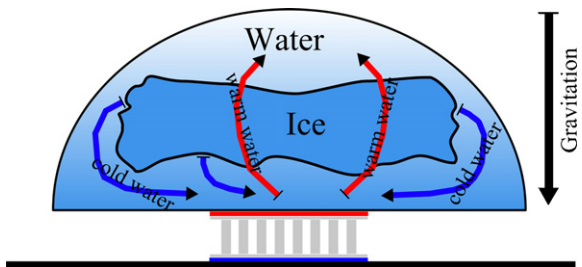


**Fig. 3.** The natural convection in the PCM causes the cold water to flow to the TEG, constantly decreasing the temperature at the TEG and thus increasing the power output compared with the convection free simulations.

liquid water has a higher density than warm water, therefore the then coldest water flows to the bottom of the containment and is located in the region close to the TEG (see Fig. 3), reducing the temperature at the device, thus increasing the temperature difference. As the simulations do not include natural convection, this specific effect is not taken into account. To support this assumption it is worth pointing out that this effect does not occur in the first part of simulated and theoretically predicted characteristics. Under these conditions, the water starts to freeze from the bottom of the containment so that natural convection plays a minor role.

#### 4. Novel TEG design

The value for the conversion  $\eta$  of heat flux into electrical energy depends on the figure-of-merit Z of the TEG:

$$\eta = \frac{[1 + Z(2T_h - \Delta T)/2]^{1/2} - 1}{[(1 + Z(2T_h - \Delta T)/2)^{1/2} + (T_h - \Delta T)/T_h]} \cdot \frac{\Delta T}{T_h} \quad (2)$$

With the definition of a device figure-of-merit  $Z_D = \alpha^2 R_{th}/R_i$ , where  $R_{th}$  is the thermal resistance of the TEG, the performance of different TEGs can be compared. First tests are done with commercial Eureca TEG1-9.1-9.9-0.8/200 [8] which offer according to the data sheet  $Z_D T$  ( $Z_D T = Z_D \cdot [T_h + T_c]/2$ ) values for the generator of 0.67 and of about 0.56 in vacuum and in air, respectively ( $R_{th,\text{vacuum}} > R_{th,\text{air}}$ ). Taking average values for  $T_h$  (=273 K) and  $\Delta T$  (=10 K)  $\eta$  is 0.41%. Considering the stored heat of  $Q = 5.04 \text{ kJ}$  [3] the theoretical electrical energy output per flight is  $W_{el} = 2 \cdot Q \cdot \eta = 41.3 \text{ J}$ . Under real operation conditions, however, thermal leakage and additional thermal resistance from the heat change material (water:  $\lambda_w \approx 0.5 \text{ W m}^{-1} \text{ K}^{-1}$ , ice:  $\lambda_i \approx 2.3 \text{ W m}^{-1} \text{ K}^{-1}$ ) occurs reducing  $\Delta T$  at the TEG, so that in pre-evaluations only an energy output of 23.3 J was achieved. These TEGs used so far are made of  $\text{Bi}_2\text{Te}_3$  and this material has a maximum ZT of 0.8 at 90 °C (see Fig. 4). To increase the conversion efficiency, a TEG from Marlow industries, inc. based on a specially doped semiconductor alloy and especially designed for the temperature range between –21.8 °C and 20.4 °C was applied. Furthermore, this device offers a voltage output of

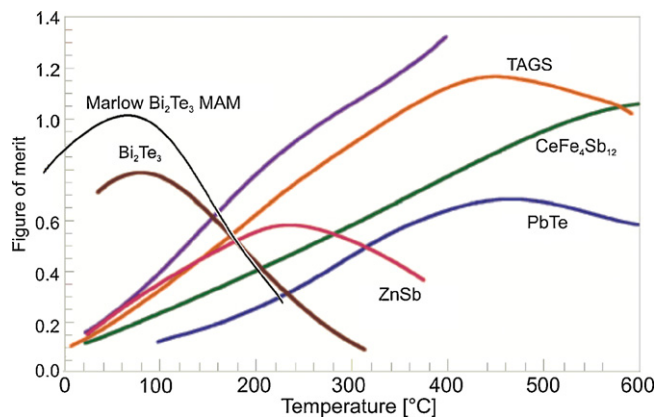


**Fig. 4.** ZT of different semiconductor alloys [9]. The improved performance of the Marlow alloy for this given application is clearly demonstrated.

**Table 1**

Comparison between theoretically predicted and experimental results of the TEGs under investigation.

TEG manufacturer	Simulation [J]	Experiment [J]	Diff sim./exp.	Improvement sim./exp.
Eureca	21.8	23.3	6.8%	
Marlow	24.8	26.5	6.8%	13.8%/13.7%

3.3 V at  $\Delta T = 20^\circ\text{C}$  with a resistive load for maximum power output ( $R_{load} \approx R_i$ ) and matches a specified  $\lambda_{TEG}$ . Enhanced ZT provides higher conversion efficiencies and a higher TEG output voltage increases the efficiency in the DC–DC converters of the power management. In the data sheet  $Z_D T$  of the Marlow TG1-2000 prototype is 0.78. According to Eq. (2), the parameter  $\eta$  is expected to be 0.53%, so that an improvement of the energy output of 29% is feasible. Under real conditions the increase will be lower as for  $\lim_{\Delta T \rightarrow 0}$  the differences in ZT become negligible. Table 1 summarizes the data gained so far. The simulation results for both the Eureca TEG and the Marlow TEG differ about 6.8% from the experimental power output for reasons explained in Section 3. But the predicted energy increase in the simulation and the experiment differs just by 0.1% demonstrating the impact of a systematic error such as the natural convection effect.

#### 5. Power-to-weight ratio

Especially for aeronautic applications the total weight of a system is an important factor. In general, the power-to-weight ratio defined as  $PtW = P/m$ , where  $P$  is the average power output of an energy source and  $m$  is its mass, influences the total weight of a system. For example, if a sensor with a power consumption of just 1 mW at the tail of the aircraft is needed and requires ten

**Table 2**

Experimental results for different PCM designs, 4 TEGs Eureca TEG1-9.1-9.9-0.2.200 and 39 Ω load resistance.

No	Short description	Energy output [J]   weight (PCM + containment, no TEG) [g]	PtW-ratio ( $t = 90 \text{ min}$ ) [ $\text{W kg}^{-1}$ ]
1	Double-walled, no internal heat pipe, 3 mounting bolts, simulation results	20.9   30.85	0.125
2	Double-walled, with internal heat pipe, 3 mounting bolts, experimental results	22.1   33.19	0.125
3	Double-walled, with internal heat pipe, 3 mounting bolts, with vacuum isolation; experimental results	23.2   33.19	0.129
4	Single-walled, with heat pipe, 2 mounting bolts, ~10 mm PU foam isolation; experimental results	30.9   27.9	0.205
5	Single-walled, with heat pipe, 2 mounting bolts, ~100 mm PU foam isolation; experimental results	35   60	0.108

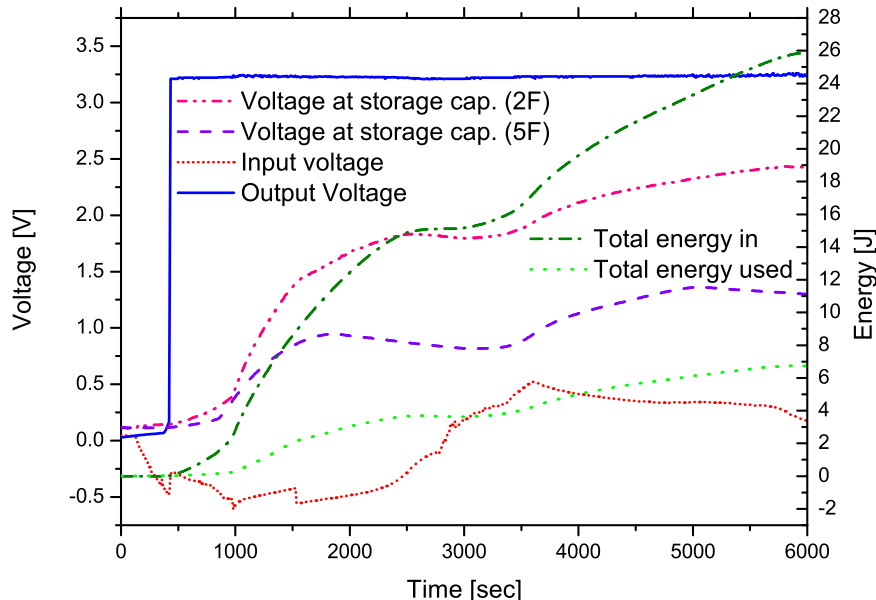


**Fig. 5.** Input/output voltages and capacitor voltage at the power management with a 2 F capacitor and energy harvesting power input from 4 Eureca TEGs. After roughly 500 s a stable 3.3 V operation voltage is provided for the sensor.

additional meters of cable to the next power line, the PtW of the cable for this sensor is  $0.001 \text{ W}/0.06 \text{ kg} = 0.017 \text{ W kg}^{-1}$ . Here, the lightest standard wire in aircraft [10], a 22 AWG copper twisted pair wire even without weight for isolation is assumed.

In such cases energy harvesting can be the superior solution and its PtW becomes important. In fact, it is even as important as the conversion efficiency of the thermoelectric energy harvester itself. Thus, the PtW ratio has to be considered as major design parameter. Yet, parameters, such as reliability or manufacturing costs, can reduce the meaning of the PtW ratio. Different designs of the PCM containment are developed and tested, resulting in a best PtW ratio so far of about  $0.205 \text{ W kg}^{-1}$  with Eureca TEGs (see also Table 2, [11]). With the expected improvement of the power output applying the new Marlow TEG of 13.7%, the PtW is expected to increase to up to  $0.23 \text{ W kg}^{-1}$ . In general, the ratio of containment mass  $m_{\text{containment}}$  and PCM material  $m_{\text{PCM}}$   $m_{\text{containment}}/m_{\text{PCM}}$  decreases for larger PCM masses, further increasing the PtW ratio.

## 6. Power management modifications

As reported in [3] and [7], several approaches were investigated how to improve the efficiency of the power management. A straight-forward improvement in the existing circuit is achieved by changing the super capacitors, which are used to store energy. The voltage level  $U$  of a capacity  $C$  depends on the stored energy according to

$$\sqrt{\frac{2W}{C}} = U \quad (3)$$

In addition, a step-up converter is used to provide a constant 3.3 V output. The efficiency of DC/DC converters depends on the input voltage [7] and selecting a capacitor which is completely charged after one flight cycle provides the highest input voltage and hence, the highest conversion efficiency. Therefore, the original 5 F storage capacitor is replaced by a 2 F device, resulting in a higher storage voltage and improved conversion performance. The conversion efficiency of the power management is here defined by

$$\eta(t) = \frac{W_{\text{used}}}{W_{\text{in}}} = \frac{\int_0^t U_{\text{node}}(t) I_{\text{node}}(t) dt + \frac{1}{2} C U_{\text{cap}}(t)^2}{\int_0^t U_{\text{in}}(t) I_{\text{in}}(t) dt} \quad (4)$$

Doing so,  $\eta$  increases from 19% (with 5 F) [3] to a total value of 26% (with 2 F) (i.e. 36% increase) although the capacity is yet not fully charged after the flight cycle and might be replaced by a 1.8 F capacitor (see also Fig. 5).

With Eq. (4), however, only a rough estimation of the conversion efficiency is possible. It is generally applicable when comparing different power management systems under laboratory test conditions with clearly defined input energies and input times. For example, in the case of the harvester presented in this article, a completely discharged power management can be measured after 6000 s simulated “flight time” in a climate chamber (see Fig. 5) and can be compared with competitive circuit boards. But, this approach has a major drawback.

Assuming the scenario that the power management has to feed a sensor node until the point of time when all its energy is consumed, the voltage at the storage capacity will decrease continuously during the discharge procedure, thereby decreasing the efficiency of the DC/DC converter. In our system with a 2 F capacity the total working time of the power management is roughly 4 h, including the 6000 s flight time in the beginning. With  $189 \mu\text{W}$  power consumption of the sensor the total efficiency is finally:

$$\eta = \frac{14,400 \text{ s} \cdot 189 \mu\text{W}}{26 \text{ J}} \approx 0.105, \quad (5)$$

much lower than the 26% predicted by Eq. (4).

The conclusion is that a proper calculation of the conversion efficiency for power management systems is not straight forward, requesting to state in detail the boundary conditions under which the conversion efficiency was measured.

## 7. Experiments of harvester and power management

In Fig. 5 the experimental results of the harvester and the power management can be seen: first, there is the low level input voltage between 0 and  $-0.7 \text{ V}$  in the first 3000 s and between 0 and  $+0.7 \text{ V}$  in the last 3000 s under electrical load. The voltage reverse results from the change in the temperature gradient at the TEG when the aircraft starts to descend. Secondly, there is the Total energy in line which represents the total amount of energy consumed by the power management. The value of 26 J in Fig. 5 is very close to that of 26.5 J gained from the experimental results



**Fig. 6.** A first prototype of a complete energy autonomous system which consists of a new microprocessor controlled power management and a sensor node (left) in combination with an energy harvester (right). All components are attached at the inside of an aircraft hull, ready for test flight validation.

with an ohmic resistor (see Table 1), showing that the power management is able to adjust its internal resistance to the optimum value for the TEGs. Additionally, it can be seen that after about 500 s the totally discharged power management is able to provide a stable 3.3 V output for the sensor node. As expected, different voltage levels result for different capacitors implemented (i.e. the smaller the capacitor, the higher the storage voltage which is the input for the output DC/DC converter). The parameter  $C$ , however, is still too large, as the critical level of 3.3 V is not fully reached. Finally, the line 'Total energy used' is the sum of stored energy in the capacitors and the consumed energy by the sensor, representing the numerator of Eq. (4).

## 8. Conclusions and outlook

In this study, a novel approach for the realization of a wireless sensor node based on a thermoelectric harvester module is presented for aircraft specific applications. In principal, two major improvements are achieved: due to the implementation of new TEGs the heat to electricity conversion is increased by about 14%, whereas the carefully adapted capacitors in the power management system added another 36% improvement in the power management. All together, this results in a theoretical increase in the conversion efficiency of about 56%. A whole system consisting of thermoelectric energy harvester, power management board and wireless sensor node with crack wire was operated under laboratory conditions for 4 h. In addition, a new management board with microprocessor controlled DC/DC converters is expected to have a total value for the power management efficiency even higher than 30%. With the numerical simulation tool different containment designs can be analyzed most efficiently, so that in a next step the weight-to-power ratio of the containment can be further optimized. Finally, a working lab demonstrator of the whole system, as shown in Fig. 6, is ready to prove its operational reliability under the harsh conditions of a test flight in the near future.

## Acknowledgement

The authors would like to thank Josh Moczygemba and Jim Bierschenk from Marlow industries, inc. for providing the sample of the TG1-2000 TEG.

## References

- [1] D. Gorinevsky, 5th International Workshop on Structural Health Monitoring, Honeywell Laboratories, Stanford, CA, September, 2005.
- [2] Bureau of Transportation Statistics, Office of Airline Information, 1200 New Jersey Avenue, SE, Washington, DC 20590, June 2009, <http://www.bts.gov/aoi>.
- [3] D. Samson, M. Kluge, Th. Becker, T. Otterpohl, U. Schmid, Energieautonomer Funknetzwerknoten für Luftfahrzeuge, E & I Elektrotechnik und Informationstechnik (in German) 127 (6) (2010) 176–180.
- [4] D. Samson, T. Otterpohl, M. Kluge, U. Schmid, Th. Becker, Aircraft-specific thermoelectric generator module, Journal of Electronic Materials, 2009 39 (9) (2010) 2092–2095.
- [5] D.W.G. Sears, J.D. Chittenden, On laboratory simulation and the temperature dependence of the evaporation rate of brine on mars, Geophysical Research Letters 32 (December) (2005) L23203.
- [6] T. Becker, M. Kluge, J. Schalk, T. Otterpohl, U. Hilleringmann, Power management for thermal energy harvesting in aircrafts 2008, IEEE Sensors Journal (26–29 October 2008) 681–684.
- [7] T. Becker, M. Kluge, J. Schalk, K. Tiplady, C. Paget, U. Hilleringmann, T. Otterpohl, Autonomous sensor nodes for aircraft structural health monitoring, IEEE Sensors Journal 9 (2009) 1589–1596.
- [8] <http://eureca.de/pdf/cooling/seebeck-elements/TEG1-9.1-9.9-0.2.100.pdf>.
- [9] G.J. Snyder, M. Christensen, E. Nishibori, T. Caillat, B.B. Iversen, Disordered zinc in  $Zn_4Sb_3$  with phonon-glass and electron-crystal thermoelectric properties, Nature materials 3 (July) (2004) 458–463.
- [10] Airbus Directives and Procedures, ABD, Airbus Industries Programmes and Processes Directorate, 31707 Blagnac CEDEX, France, 2001.
- [11] D. Samson, M. Kluge, Th. Becker, U. Schmid, Optimization of a heat storage device for an aircraft specific thermoelectric power generator, Proceedings of the ECT (2010) 115–119.

## Biographies

**Dominik Samson** was born in Saarbrücken, Germany in 1984. He studied physics at the Saarland University from 2003 to 2008 and left university with a diploma degree in physics. 2008 he entered EADS Innovation Works to do his PhD on energy harvesting in aircraft. His main working field is the thermoelectricity.

**Martin Kluge**, born in 1976, he studied Engineering Physics at the University of Applied Sciences in Munich and graduated with a German Diplom-Ingenieur (FH) degree in April 2001. Ever since he is working as a research engineer for EADS Innovation Works. From 2001 to 2004 his main occupation was research in the field of MEMS inertial sensors. Since 2004 he is working in the field of electronics and integration with focus on wireless sensors, energy harvesting and packaging.

**Prof. Dr. Thomas Becker** graduated (Dipl.-Ing.) in electrical engineering in 1995 and he received his doctoral level (Dr.-Ing.) from the University of Bremen, Germany. In 1994 he joined EADS Innovation Works, formerly DaimlerChrysler Research and Technology, in Munich, Germany. From 2002 to 2004 he has been acting as Key Technology Area Manager for Microsystems, Electronics and Microelectronics. In 2004 he has been appointed as Manager for Gas Sensor Systems and in 2010 as Expert for Autonomous Sensor Systems. Since 2003 he is also guest lecturer at the private University of Applied Science in Isny/Germany (NTA). In 2008 he became Adjunct Professor and he is President of the sponsoring society (FöVe) of the NTA. He is author and co-author of about 70 publications in textbooks, scientific journals and conference proceedings and he holds about 25 patents or pending patents. He also served as chairman for several international conferences.

**Prof. U. Schmid** was born in Munich, Germany, in 1972. He started studies in physics and mathematics at the University of Kassel in 1992. In 1995, he spent 6 months at the Transport Group in the Physics Department, University of Nottingham, UK, to gain experience in wide band gap semiconductor physics. He performed his diploma work at the research laboratories of the Daimler-Benz AG (now DaimlerChrysler AG) on the electrical characterization of silicon carbide (6H-SiC) microelectronic devices for high temperature applications. He finished his studies in 1998 at the University of Frankfurt/Main, Germany. In 1999, he joined the research laboratories of DaimlerChrysler AG (now EADS Deutschland GmbH) in Ottobrunn/Munich, Germany. He developed a robust flow sensor for high-pressure automotive applications and received his Ph.D. degree in 2003 from the Technical University of Munich, Germany. From 2003 to 2008, he was post-doc at the Chair of Micromechanics, Microfluidics/Microactuators at Saarland University. Since October 2008, he is full professor at the Vienna University of Technology heading the Department for Microsystems Technology. U. Schmid holds 14 patents and has authored or co-authored more than 130 publications in refereed journals and conferences.